sustainability

MDPI

Article

Application of Novel Biochar Derived from Experimental Sewage Sludge Gasification as an Adsorbent for Heavy Metals Removal

Domagoj Nakić *, Hana Posavčić, Katarina Licht and Dražen Vouk

Faculty of Civil Engineering, University of Zagreb, 10 000 Zagreb, Croatia;
hana.posavcic@grad.unizg.hr (H.P.); katarina.licht@grad.unizg.hr (K.L.); drazen.vouk@grad.unizg.hr (D.V.)
* Correspondence: domagoj.nakic@grad.unizg.hr

Abstract: The growing amounts of sewage sludge (SS) and water pollution caused by heavy metals are major environmental concerns. This study addresses both issues by investigating the potential of biochar derived from SS gasification at an experimental plant as an effective adsorbent for the removal of selected heavy metals, cadmium, chromium, copper, and lead, from synthetic wastewater. A Box–Behnken design was used to determine the influence of the biochar mass, initial heavy metal concentration, pH, and time on the heavy metal removal. For the statistical analysis, 104 experiments were performed. The pristine SS biochar demonstrated an adsorption capacity reaching up to 46.64 mg/g for Cd, 43.89 mg/g for Cr, 42.42 mg/g for Cu, and 72.66 mg/g for Pb from single-component synthetic solutions in acidic-to-neutral conditions, with an over 99% removal efficiency for all four heavy metals under optimal conditions. The removal of all the tested metals followed pseudo-second-order kinetics, with Cd fitting the Langmuir model and Pb, Cr, and Cu fitting the Freundlich model. This paper also provides suggestions for further research focused on the multiple uses of biochar as an adsorbent and later as a substitute material in the construction industry, aiming to achieve an integrated approach and maximizing the overall sustainability of wastewater treatment and waste management by utilizing waste as a resource.

Keywords: sewage sludge; gasification; biochar; adsorption; wastewater treatment; heavy metals; cadmium; chromium; copper; lead

Academic Editor: Andreas Angelakis

Received: 3 January 2025
Revised: 23 January 2025
Accepted: 24 January 2025
Published: 26 January 2025

Citation: Nakić, D.; Posavčić, H.; Licht, K.; Vouk, D. Application of Novel Biochar Derived from Experimental Sewage Sludge Gasification as an Adsorbent for Heavy Metals Removal. *Sustainability* **2025**, *17*, 997. https://doi.org/10.3390/su17030997

1. Introduction

In recent years, stricter wastewater treatment and discharge standards have been introduced, driving the growth of wastewater treatment plants (WWTPs) and leading to increased sewage sludge (SS) production. As the efficiency of urban WWTPs improves, SS production has correspondingly increased. The global production of SS in 2017 was estimated at 45 million tons of dry solids and is projected to reach 127.5 million tons by 2030 [1]. The data for the EU27 estimate the annual production of SS at about 10 million tons of dry solids [2]. The increasing volume of SS production, along with rising treatment costs and stricter standards, underscores the urgent need to explore methods for reducing sludge accumulation and promoting its resource utilization. In the European Union, the main treatment methods are biostabilization, dewatering, and drying. Over 50% of SS is stabilized by anaerobic digestion. Its final disposal mainly involves land application or

resource recovery after incineration, with landfill use declining. In the US, nearly 60% of SS is stabilized by aerobic composting or anaerobic fermentation and is used as a biomass fertilizer, while the remainder is incinerated, landfilled, or used for mine rehabilitation. In Japan, SS treatment relies on anaerobic digestion, composting, and melting, with recent disposal methods focusing on its harmless use in gardens or green spaces, and the incineration ash being converted into bricks or building materials [3]. Transforming SS into a resource is a growing trend in these areas and globally. The EU Directive 91/271/EEC promotes sustainable SS management through recycling and reducing its environmental impacts. For SS unsuitable for agriculture, thermal treatments like gasification, pyrolysis, and hydrothermal carbonization are effective options, converting sludge into biochar. These methods reduce waste volume, eliminate microorganisms, and transform organic matter into valuable byproducts [4–7].

While conventional incinerators are used for large-scale systems due to their energy efficiency, gasification is well suited for decentralized systems as it reduces greenhouse gas emissions [8]. Gasification eliminates SS, removes pollutants, and generates energy with lower emissions and reduced migration of heavy metals [9]. At temperatures above 800 °C, it converts SS into syngas, biochar, and ash [8]. Biochar from organic waste, a carbon-rich porous material with an aromatic compound structure [9], can be used in wastewater treatment due to its high adsorption capacity [4,5,10–12]. Biochar produced at higher temperatures has enhanced porosity, and heavy metal leaching is minimal [4].

Another distinct environmental issue is heavy metals in aquatic systems, which pose significant environmental, ecological, and public health risks due to their environmental persistence and non-biodegradable nature. Lead, chromium, copper, and cadmium are among the most concerning heavy metals due to their toxicity and prevalence in wastewater. Cadmium, for instance, is particularly concerning, being common in drinking water and wastewater and considered one of the most toxic pollutants [13]. Therefore, removing heavy metals from wastewater is a critical issue, and among the various methods, adsorption has proven to be an effective approach. Previous research has shown that the efficiency of heavy metal ion adsorption by SS-based biochar is highly influenced by the chemical activator used during its modification, where the choice of the activator plays a crucial role in enhancing a material's adsorption capacity [14].

This paper explores biochar from SS gasification as an adsorbent for the removal of heavy metals in wastewater treatment. Previous studies have shown SS-derived biochar effectively adsorbs metals like Pb(II), Cd(II), Cr(VI), As(III), Cu(II), Zn(II), and Ni(II), and helps remediate contaminated soils [7,15]. Singh et al. [16] reviewed the preparation, activation, and adsorption methods for SS-derived biochar, highlighting its potential as an adsorbent alongside activated carbon. However, these processes often yield biochar with a low surface area and poor pore structure due to SS's limited carbon content, which are essential for effective adsorption [17,18].

The effectiveness of biochar at removing heavy metals depends on factors, such as the biomass type, modification methods, gasification or pyrolysis conditions, solution pH, coexisting ions, temperature, and adsorbent dosage [19]. The key adsorbent properties include high selectivity and capacity, low cost, stability, and longevity. The chemical composition, surface area, ash content, and functional groups in biochar influence its adsorption properties. Modifications with reagents like $Ca(OH)_2$, $MgCl_2$, $ZnCl_2$, and KOH create rougher, more heterogeneous surfaces [16,20]. Pristine SS-based biochar often shows low performance, limiting its practical use. Chemical treatments and modifications of the pyrolysis/gasification conditions improve biochar properties and its pollutant-removal capacity. Lin et al. [21] conducted adsorption experiments on Cu^{2+} and Pb^{3+} using different chemical activators (KOH, $ZnCl_2$, and H_3PO_4) to modify SS-based biochar. They found that KOH modification at 600 °C produced the largest specific surface area, but H_3PO_4-

modified biochar had the best adsorption capacity for Cu^{2+} and Pb^{3+}. Kang et al. [22] demonstrated that nano-zero-valent iron-supported SS biochar outperformed unmodified sludge biochar at removing Cu(II) and Cr(VI) during heavy metal removal experiments, with maximum adsorption capacities of 215.40 mg/g for Cu(II) and 177.10 mg/g for Cr(VI). The heavy metal interaction experiment showed that Cr(VI) and Cu(II) competed for the active sites, with Cr(VI) being more easily absorbed by the biochar. Despite its potential, SS-based biochar may be less attractive in the potential market than other types with better adsorption properties. In addition to environmental risks and applicability concerns, commercial challenges may arise from economic and social viability issues. Cao et al. [14] concluded that the co-pyrolysis of SS and biomass produces biochar with better adsorption properties, making it a promising material for treating wastewater contaminated with pollutants like dyes, heavy metals, drugs, and pesticides.

A literature review of studies on SS biochar for water contaminant removal shows significant variations in the results: Liu et al. [23] reported a Cr(VI) adsorption capacity of 11.6 mg/g for biochar produced from nano-zero-valent iron and SS; Wang et al. [24] found removal efficiencies for Pb, Cu, and Zn of 21.3%, 72.1%, and 30.3%, respectively; Zhang et al. [25] reported removal efficiencies for Cr, Cu, and Zn of 77.0%, 97.4%, and 99.7%, respectively; and Zhu et al. [26] found a Cr(VI) adsorption capacity of 22.9 mg/g for SS biochar. Usman et al. [19] also concluded, based on a comprehensive literature review, that modified biochar performs substantially better than pristine biochar for pollutant adsorption. Despite numerous studies on SS-based biochar for pollutants like heavy metals, the high modification costs and waste treatment hinder its large-scale use [27]. The use of unmodified biochar for the removal of heavy metals remains underexplored, which this paper aims to address. While surface modification boosts adsorption capacity, it is costly and energy-intensive. SS-derived biochar offers dual benefits: an abundant feedstock (SS) and an effective waste management solution [13].

The literature review reveals that, despite the increasing number of studies on biochar as an adsorbent, there are still gaps to be addressed. One such area is the potential use of SS biochar produced through new or modified thermochemical decomposition technologies, such as the experimental gasification plant used to obtain the biochar in this research.

The primary aim of this study is to assess the effectiveness of pristine biochar, derived from a specialized gasification process for SS in an experimental plant, at removing selected heavy metals from synthetic wastewater. This experimental gasification plant developed in Croatia focuses on producing hydrogen-rich synthetic gas from various wastes, including SS. The main challenge is managing the residual biochar. While biochar has been successfully used in concrete [28] and brick production [29] as a partial raw material replacement, its potential as an adsorbent for heavy metals removal from wastewater is now being explored. Despite concerns about secondary pollution from the desorption of heavy metals or organic matter, the initial findings have suggested this is unlikely [30–32], supporting its reuse in multiple applications.

2. Materials and Methods

2.1. Origin and Process of Biochar Production

Since there are no full-scale gasification plants in Croatia, the biochar used in this study was obtained by gasifying SS at an experimental plant. The SS was sampled from a tertiary WWTP in Croatia, dried at 105 °C, and subjected to the gasification process in the aforementioned experimental plant (as shown in Figure 1). The gasification plant converts solid organic material into clean syngas and inert residue. It operates with an input waste capacity of approximately 50 kg/h, resulting in around 50% inert residue (biochar) as the output during the gasification of used SS. The process occurs in a reactor, where the

syngas reaches up to 850 °C. The syngas contains 45–60% hydrogen, suitable for various applications. By-products, such as fly ash and bottom bed residue (biochar), can be used in construction or wastewater treatment. This plant's innovations include superheating the syngas, reducing the reactor's thermal load by separating the superheater, and recovering internal heat from the syngas. This waste-to-syngas technology minimizes CO_2 and other harmful emissions by maintaining high temperatures and preventing oxygen from entering the process. The operating principle of the experimental plant is described in detail by Bubalo et al. [33]. One of the remaining challenges is managing the residual biochar. In this study, the biochar was further analyzed and used as an adsorbent for treating synthetic wastewater containing selected heavy metals.

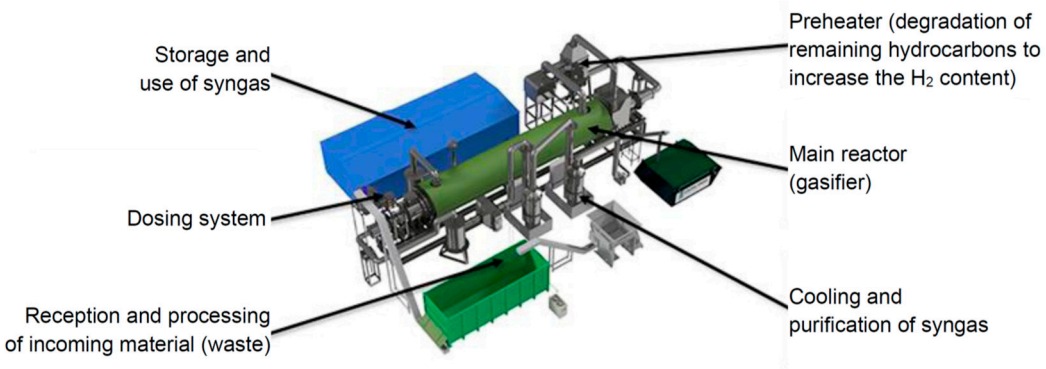

Figure 1. Schematic of the experimental gasification plant from which the biochar used in this study was obtained [33].

2.2. Biochar Characterization

The biochar's chemical composition was determined by atomic absorption spectroscopy (Analyst 200, PerkinElmer, USA). Samples were dissolved in aqua regia and hydrofluoric acid in a Teflon-lined steel autoclave, then diluted, and measured as oxide mass fractions.

The biochar sample was also analyzed by energy-dispersive X-ray fluorescence (EDXRF, Siemens X-ray tube with Mo anode and Mo secondary target). Element concentrations were determined using IAEA QXAS software by comparing counting rates with the IAEA-SL-1 reference material [29].

The morphology of the biochar was examined using scanning electron microscopy (SEM, Tescan Vega 3). Samples were chromium-coated for 100 s with a Q150T evaporator (Quorum Technologies, UK). Micrographs were captured at 8 kx and 20 kx magnifications with 5 and 2 μm resolutions.

Leaching tests followed the EN 12457 standard: "Characterisation of waste - Leaching - Compliance test for leaching of granular waste materials and sludges.". About 90 g of biochar was mixed with demineralized water (L/S = 10) in a 1 L glass vessel and agitated at 2 rpm for 24 h. After settling for 15 ± 5 min, the eluate was vacuum-filtered (0.45 μm). For heavy metal analysis by atomic absorption spectrometry (Perkin Elmer Analyst 800), 1 mL of 65% nitric acid per 100 mL of filtrate was added. The procedure is described in detail by Nakić et al. [34].

In order to determine the pH of zero point of charge (pH_{ZPC}), the salt addition method was used. A total of 50 mL of 0.1 M NaCl was added to a series of flasks and the pH of the solution was adjusted within a range from 2 to 12 using 1 M NaOH and HCl. After adding 0.1 g of biochar to each flask, they were agitated for 48 h, after which final pH of the suspensions was measured. The pH_{ZPC} was determined by plotting the difference between final and initial pH (ΔpH) against initial pH. The intersection point of the initial pH and ΔpH curves on the graph indicates the pHzpc value.

2.3. Procedure for Conducting Adsorption Batch Experiments

The experiments were carried out according to the experimental matrix shown in described in 3.2 Experimental design. All reagents used in the experiments and analyses were of analytical grade. Stock solutions of heavy metals for the adsorption experiments were prepared by dissolving appropriate amounts of analytical-grade cadmium nitrate ($Cd(NO_3)_2$), copper nitrate ($Cu(NO_3)_2$), lead nitrate ($Pb(NO_3)_2$), and chromium nitrate ($Cr(NO_3)_3$) in deionized water. Working solutions of 20, 110, and 200 mg/L were prepared by diluting the stock solutions with deionized water. The pH of each solution was adjusted to 3, 5, or 7 using 0.1 M HCl or 0.1 M NaOH. pH measurements were taken with a HI98194 multiparameter (Hanna Instruments, USA).

Adsorption experiments were performed in 250 mL sealed bottles containing 100 mL of heavy metal solution and specified amounts of biochar (0.25, 0.50, or 0.75 g). The bottles were placed on an overhead shaker (Reax 2, Heidolph, Germany) and agitated at 45 rpm at room temperature (approximately 25 °C) for the specified contact times (6, 15, or 24 h).

Following the adsorption period, the samples were filtered through a 0.45 µm syringe filter to separate the biochar. Residual concentrations of cadmium, copper, lead, and chromium in the filtrate were determined using an inductively coupled plasma optical emission spectrometer (ICP-OES) (Agilent 5900, Agilent Technologies, USA). All experiments were performed in triplicate, and the average values were used to calculate the amount of adsorbate adsorbed by the biochar, as presented in the results. The adsorbed amount was calculated using Equation (1):

$$q_t = V \frac{C_0 - C_t}{m} \quad (1)$$

where q_t (mg/g) represents the amount of adsorbate adsorbed per gram of biochar; C_0 and C_t (mg/L) are the initial and final concentrations of the adsorbate in the solution, respectively; V (L) is the solution volume; and m (g) is the weight of the adsorbent used.

3. Results

3.1. Properties of the Produced Biochar

The biochar produced consists of various high-temperature aluminosilicates, primarily quartz and cristobalite (SiO_2), with notable amounts of illite and traces of calcite ($CaCO_3$) and calcium aluminum phosphate. Its calcium-based crystalline composition suggests a possible solid–solution formation due to the isostructural similarity among the phases. The sample shows overlapping weak-intensity maxima, complicating the identification of the less abundant components, and contains no amorphous phase. The absorption spectrometry analysis revealed that the biochar sample's major components are Al_2O_3 (~16%), CaO (~15%), and Fe_2O_3 (~11%), with nearly half (48%) of the mass remaining undissolved, attributed to biochar carbon (Figure 2).

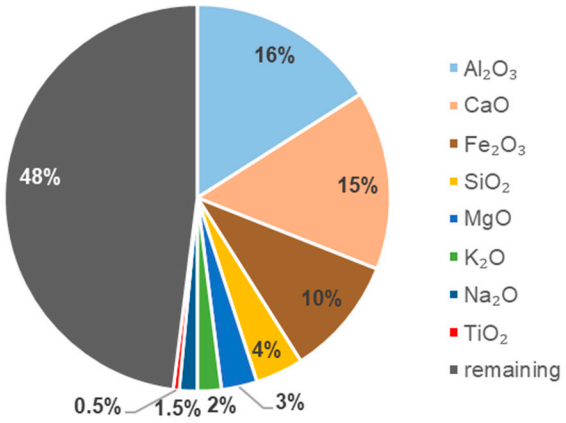

Figure 2. Chemical composition of the produced biochar by absorption spectrometry analysis.

The most toxic heavy metals typically found in SS include arsenic, lead, mercury, and cadmium. These metals are non-biodegradable, which leads to their accumulation. Even at low concentrations, they can dissolve and contaminate the environment, underscoring the need for the safe disposal of waste containing them, including wastewater [33]. The content analysis of the key problematic elements, including heavy metals, in the biochar is shown in Figure 3, which is generally in agreement with the results of other studies (such as [13], where these values ranged from 12.36 mg/kg for Cd to 2510 mg/kg for Mn), or indicates slightly lower concentrations of heavy metals in this biochar. The overall results show low levels of hazardous metals in the biochar, and the sedimentation from alkaline substances (especially Ca components) and phosphates will further reduce the leachate toxicity below safety thresholds, enabling its safe application for various purposes [35].

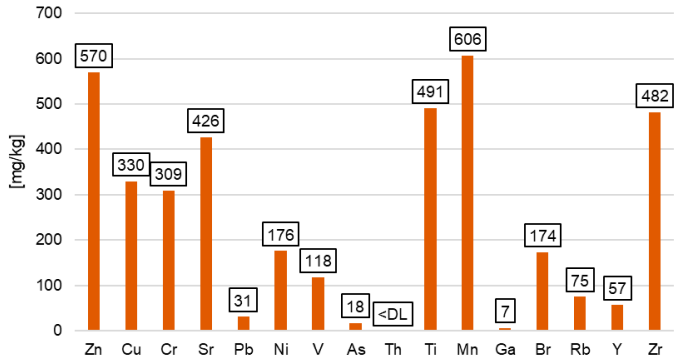

Figure 3. Analysis of the content of heavy metals and other potentially hazardous elements in the obtained biochar (DL—detection limit).

Leaching tests are used to determine the concentration of elements (mainly heavy metals) released from the solid to the liquid phase over time, assessing their potential hazard and bioavailability. In this study, leaching tests were conducted following the EN 12457 standard, which is used for classifying waste for landfill disposal (hazardous, non-hazardous, or inert). The tests aimed to identify the potentially hazardous elements and the application limitations of this biochar. The results are shown in Table 1.

Table 1. Leaching test results of the produced biochar according to EN 12457 [mg/kg].

Heavy Metal	Biochar Sample
As	<DL
Ba	10.600
Cd	<DL
Co	0.005
Cr	0.350
Cu	<DL
Mo	0.800
Ni	<DL
Pb	0.008
Se	0.006
Zn	<DL

DL—detection limit.

The relative solubility of each metal can be estimated by comparing the leaching results with the initial heavy metal content of the biochar. The leaching concentrations are extremely low, with some being undetectable, except for Mo, which shows moderate leaching. Zn and Pb exhibit very low solubility, as do As, Cd, Cu, and Ni, while Cr has a low but noticeable solubility. Mo shows high solubility, though the total leaching remains low due to its initially low concentration. Similar trends have been reported in previous studies [34,36]. These findings support the conclusion of Zielinska et al. [37] that, overall, heavy metals in SS-derived biochar are stable, minimizing the contamination risks during application. So, the main conclusion is that using biochar as an adsorbent in wastewater treatment is expected to be feasible and safe, with no significant release of hazardous substances into the treated water. Several authors have explained this phenomenon, suggesting that the metals present in SS are trapped in the biochar matrix pores or react with the inorganic mineral components of the biomass to form more stable co-crystal compounds, thereby reducing the toxicity of the heavy metals [14,38,39]. Issues related to the release of heavy metals or other problematic compounds are not initially expected based on the conducted leaching tests. However, this issue undoubtedly requires further confirmation, especially through repeated cycles using the same biochar sample.

Figure 4 shows the SEM micrographs of the biochar with poly-dispersed grains and irregularly shaped, rugged particles. The particles are agglomerated, forming a rough and porous isomorphic mass with a network of small cavities and voids. This structure provides a large surface area and numerous active sites. The varying pore sizes and shapes may influence the adsorption performance by affecting how the adsorbate reaches the active sites. These pores are believed to play a key role in the adsorption of metal ions onto the adsorbent's surface.

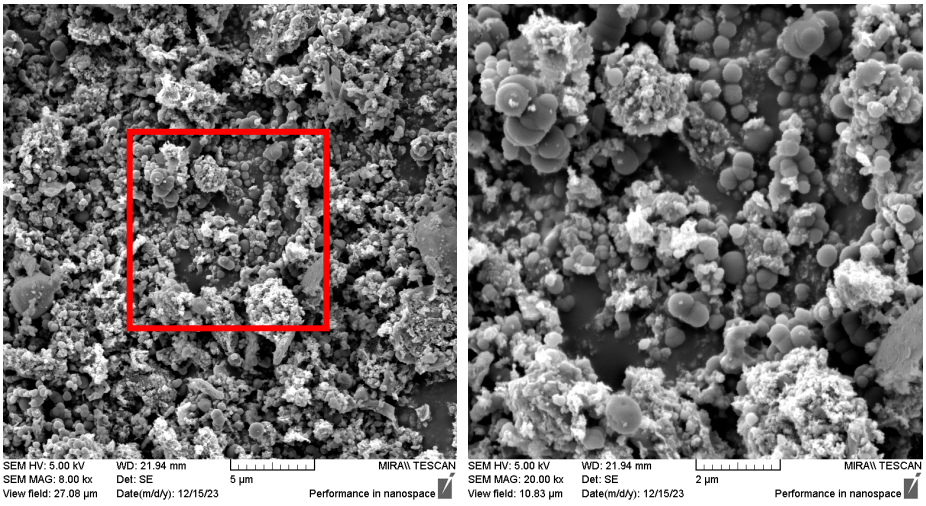

Figure 4. SEM images of the obtained biochar at varying magnification levels.

The point of zero charge for this biochar is estimated to be around 10.5 based on the experimental data. This value indicates the pH at which the biochar's surface carries no net electrical charge. Below this pH, the biochar surface is predominantly positively charged, enhancing its ability to adsorb anions. Above the pHzpc, the surface becomes negatively charged, favoring the adsorption of cations.

3.2. Experimental Design

With the use of the Response Surface Methodology (RSM) in the Design-Expert software, a series of experiments was conducted. The aim was to obtain the optimum multifactorial operating conditions for the adsorption of different heavy metals. A Box–

Behnken design (BBD) for four factors was chosen as the experimental design as it requires three levels for each factor, all within the specified operating range. Therefore, each of the four factors is distributed at one of the three levels (low (−1), medium (0), and high (+1)) [40].

The four numerical factors included the biochar mass (A), pH (B), initial heavy metal concentration (C), and time (D). The factors and their value ranges are listed in Table 2.

Table 2. Ranges of factors.

Factor (Unit)	Levels		
	−1	**0**	**1**
(A) Biochar mass (g)	0.25	0.5	0.75
(B) pH	3	5	7
(C) Initial heavy metal concentration, c_{in} (mg/L)	20	110	200
(D) time (h)	6	12	24

After determining the factors and their levels, an experimental matrix with a total of 26 test series was created. These series were analyzed for each heavy metal, including Cd, Cr, Cu, and Pb. Thus, a total of 104 experiments were performed. The matrix is shown in Table 3 together with the experimental ($y_{exp.}$) and predicted ($y_{pred.}$) values of the responses. The calculated adsorption capacities (q_t) for each heavy metal are also included in this table. Model graphs (3D response surface plots) were created to clearly illustrate the interactions between the independent variables and their combined effect on the response.

Table 3. Experimental matrix with experimental and predicted values of heavy metal removal efficiency and calculated adsorption capacities.

Run	A: Biochar Mass (g)	B: pH	C: c_{in} (mg/L)	D: Time (h)	Cd $y_{exp.}$ (%)	Cd $y_{pred.}$ (%)	q_t (Cd) (mg/g)	Cr $y_{exp.}$ (%)	Cr $y_{pred.}$ (%)	q_t (Cr) (mg/g)	Cu $y_{exp.}$ (%)	Cu $y_{pred.}$ (%)	q_t (Cu) (mg/g)	Pb $y_{exp.}$ (%)	Pb $y_{pred.}$ (%)	q_t (Pb) (mg/g)
1	0.25	5	110	6	60.34	60.62	26.55	9.25	43.40	4.07	40.48	64.71	17.81	94.89	96.83	41.75
2	0.75	5	110	6	99.89	102.3	14.65	97.34	90.78	14.28	99.51	99.07	14.59	95.87	94.96	14.06
3	0.5	3	20	15	99.30	95.03	3.97	99.90	76.13	4.00	99.95	93.49	4.00	98.95	94.03	3.96
4	0.5	7	20	15	99.80	108.9	3.99	99.80	110.04	3.99	99.90	113.22	4.00	97.35	91.53	3.89
5	0.5	7	200	15	99.13	95.82	39.65	99.99	83.06	40.00	66.75	70.30	26.70	97.94	96.89	39.18
6	0.75	5	20	15	99.60	95.98	2.66	99.80	116.78	2.66	99.90	120.53	2.66	83.60	85.84	2.23
7	0.5	3	110	24	99.90	94.91	21.98	93.82	75.13	20.64	99.92	72.03	21.98	98.51	100.03	21.67
8	0.75	7	110	15	99.93	95.72	14.66	99.97	95.98	14.66	99.99	93.73	14.67	96.00	96.60	14.08
9	0.25	5	20	15	99.35	92.86	7.95	99.75	69.39	7.98	98.40	86.17	7.87	92.05	93.95	7.36
10	0.5	5	110	15	99.90	95.43	21.98	94.65	79.59	20.82	94.97	81.89	20.89	99.45	95.90	21.88
11	0.5	3	200	15	80.54	81.95	32.22	46.20	49.14	18.48	39.43	50.57	15.77	98.23	99.39	39.29
12	0.75	5	200	15	99.88	103.57	26.63	97.85	89.79	26.09	83.55	77.61	22.28	94.87	97.44	25.30
13	0.25	5	110	24	96.13	91.36	42.30	54.58	68.40	24.02	64.06	64.71	28.19	99.42	96.83	43.74
14	0.5	7	110	6	99.84	95.94	21.96	94.04	84.05	20.69	99.86	91.76	21.97	92.82	97.53	20.42
15	0.5	7	110	24	99.98	108.78	22.00	99.26	109.05	21.84	99.86	91.76	21.97	95.19	97.53	20.94
16	0.75	5	110	24	99.86	97.24	14.65	99.97	115.78	14.66	99.50	99.07	14.59	97.16	94.96	14.25
17	0.5	5	20	6	98.15	95.55	3.93	99.95	80.59	4.00	99.45	103.35	3.98	87.95	89.90	3.52
18	0.25	7	110	15	93.13	93.92	40.98	99.75	97.12	43.89	96.40	89.79	42.42	99.25	98.47	43.67
19	0.5	5	110	15	99.99	95.43	22.00	46.76	79.59	10.29	99.97	81.89	21.99	99.23	95.90	21.83
20	0.25	5	200	15	58.30	59.12	46.64	44.55	42.41	35.64	41.39	43.25	33.11	90.82	93.06	72.66
21	0.25	3	110	15	48.70	58.06	21.43	2.34	14.68	1.03	32.25	39.64	14.19	79.85	82.03	35.13

22	0.5	5	200	24	99.98	95.31	39.99	99.55	78.60	39.82	62.29	60.43	24.91	98.07	95.25	39.23
23	0.5	5	20	24	99.45	108.39	3.98	97.05	105.58	3.88	95.95	103.35	3.84	85.25	89.90	3.41
24	0.5	3	110	6	80.67	82.07	17.75	47.47	50.13	10.44	76.17	72.03	16.76	98.20	100.03	21.60
25	0.5	5	200	6	79.36	82.47	31.74	46.19	53.60	18.48	42.63	60.43	17.05	97.37	95.25	38.95
26	0.75	3	110	15	99.46	103.83	14.59	99.58	110.58	14.61	96.67	104.41	14.18	98.69	99.10	14.47

3.3. Results of Adsorption Experiments

3.3.1. Analysis of Variance (ANOVA)

Statistical testing of the model was carried out using the statistical test Analysis of Variance (ANOVA). The results of the ANOVA for the removal of Cd, Cr, Cu, and Pb are shown in Table 4. The ANOVA for these responses shows that the models are significant due to the low probability value ($p < 0.0001$). In general, models with a *p*-value of less than 0.1 are considered statistically significant.

The df values (degrees of freedom) indicate the number of factors included in the model. For example, in the case of Cd removal, eight factors are included, A, B, C, D, AB, AC, AD and A^2, as their *p*-values are less than 0.1, which means that these factors are significant. The factors with *p*-values above 0.1 are mainly excluded. For example, for the adsorption of Cu and Pb, the factor D—time—is excluded from further analysis. In general, this means that the available data do not provide evidence of an effect. It can also mean that a variable has no influence on the response (adsorption), or that the sample size is too small, or that the variable is correlated with other variables and its contribution to the process is not defined. In the case of Pb, the *p*-value for the variable A—biochar mass—is 0.3615 and is retained to ensure the model's hierarchy.

Table 4. ANOVA for reduced linear model.

Source	Sum of Squares	df	Mean Square	F-Value	*p*-Value
Cd removal					
Model	4880.45	8	610.06	16.66	<0.0001
A—biochar mass	1696.55	1	1696.55	46.34	<0.0001
B—pH	577.15	1	577.15	15.76	0.001
C—c_{in}	513.13	1	513.13	14.02	0.0016
D—time	494.69	1	494.69	13.51	0.0019
AB	483.2	1	483.2	13.2	0.0021
AC	427.15	1	427.15	11.67	0.0033
AD	320.57	1	320.57	8.76	0.0088
A^2	368.03	1	368.03	10.05	0.0056
Cr removal					
Model	16,600.2	5	3320.04	9.5	<0.0001
A—biochar mass	6735.13	1	6735.13	19.27	0.0003
B—pH	3451.47	1	3451.47	9.88	0.0051
C—c, in	2185.25	1	2185.25	6.25	0.0212
D—time	1874.78	1	1874.78	5.37	0.0313
AB	2353.57	1	2353.57	6.74	0.0173
Cu removal					
Model	11,160.81	4	2790.202	16.41202	<0.0001
A—biochar mass	3541.032	1	3541.032	20.82842	0.000169
B—pH	1167.702	1	1167.702	6.868446	0.015972
C—c_{in}	5526.808	1	5526.808	32.50879	<0.0001
AB	925.2658	1	925.2658	5.442431	0.029679
Pb removal					
Model	279.99	6	46.66	4.35	0.0069

A—biochar mass	9.4	1	9.4	0.8766	0.3615
B—pH	16.8	1	16.8	1.57	0.2266
C—c_{in}	86.05	1	86.05	8.03	0.011
AC	39.03	1	39.03	3.64	0.0724
B^2	48.69	1	48.69	4.54	0.0471
C^2	65.68	1	65.68	6.13	0.0235

3.3.2. Cadmium Removal Efficiency

The mathematical equation below can be used to make predictions about Cd adsorption. This is the equation in terms of the actual factors, and the values should be given in the original units for each factor from Table 2.

$$Y = -38.1222 + 287.383A + 14.4585B - 0.302296C + 2.70277D - 21.9818AB + 0.459278AC - 3.97875AD - 120.752A^2 \quad (2)$$

The normal plot of the residuals is shown in Figure 5. The residuals are normally distributed as they mostly fall close to the straight line. Therefore, the plot indicates that the model is valid.

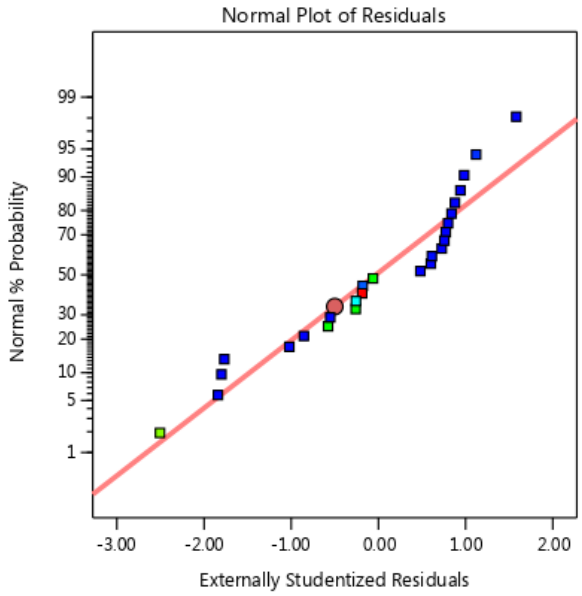

Figure 5. Normal plot of residuals for Cd removal efficiency.

The contour plot and the 3D response surface in Figure 6 show different interactions in terms of Cd removal efficiency.

Three levels of the adsorbent dose (biochar mass) were investigated (0.25, 0.5, and 0.75 g). As expected, a higher biochar mass resulted in higher Cd adsorption (Figure 6(top)). In the study by Chen et al. [41], Cd removal increased up to 100% when the biochar dosage was increased to 125 mg/L, after which equilibrium was reached.

The pH of a solution is considered one of the most important parameters affecting metal adsorption. It can influence the adsorption performance in several ways: through electrostatic repulsion between the adsorbent and adsorbate, through ion exchange, and through the distribution of metal species [41]. Increasing the pH value had a positive effect on Cd adsorption. However, when using 0.60 g of biochar or more, the pH had no significant effect on Cd removal. Similar results were obtained by Chen et al. [41], who also found that Cd removal efficiency increased with an increasing initial pH. They reached equilibrium at pH 4.

The results observed from the variations in the initial Cd concentration (Figure 6 (middle)) show that higher removal efficiencies are achieved with lower initial concentrations. However, with 0.55 g of biochar or more, even the highest initial concentrations of Cd can be removed. This suggests that biochar has a significant capacity for Cd adsorption, and that this capacity is less sensitive to variations in the initial Cd concentrations when higher amounts of biochar are used.

The interaction between the initial biochar mass and time (Figure 6 (bottom)) shows that Cd adsorption increases linearly with the duration of treatment. Notably, when using 0.60 g of biochar or more, the required treatment time for effective Cd removal is markedly reduced. For instance, achieving 95% Cd removal takes 24 h with 0.35 g of biochar, whereas only 6 h are needed when using 0.60 g of biochar. This highlights the efficiency of larger biochar amounts for accelerating the adsorption process.

From all this, it can be concluded that the highest Cd adsorption can be achieved after 6 h when using 0.60 g of biochar, regardless of the initial concentration (20–200 mg Cd/L). This is suggested as the optimal combination of biochar mass and treatment duration that maximizes removal efficiency across a broad range of Cd concentrations.

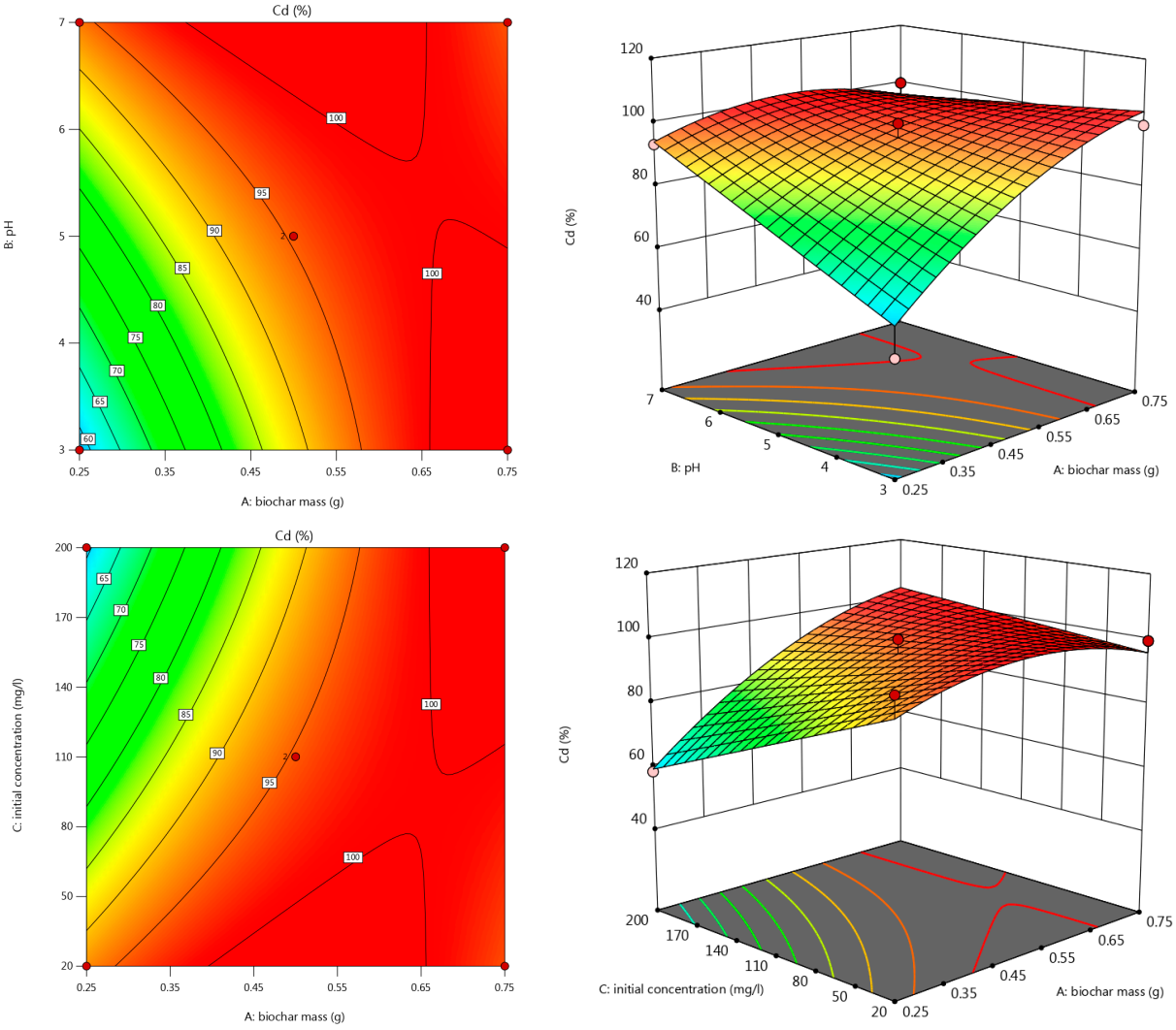

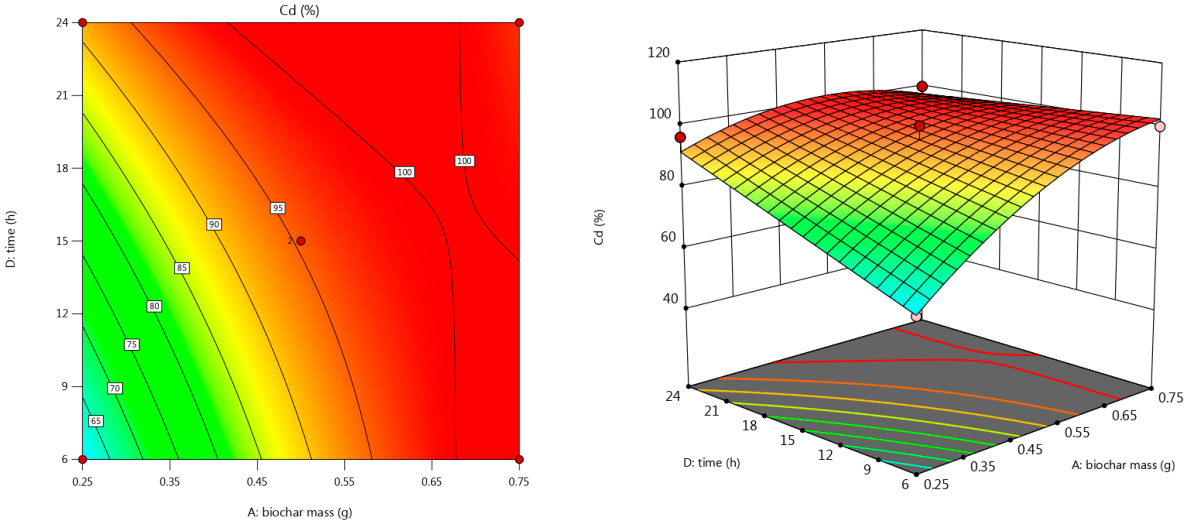

Figure 6. Contour plot (**left**) and 3D response surface (**right**) for combined effect of pH and biochar mass (**top**); initial Cd concentration and biochar mass (**middle**); time and biochar mass on Cd removal (**bottom**).

The adsorption capacity of Cd (Table 3) varies between 2.66 mg/g and 46.6 mg/g, depending on the experimental setup. Compared to similar studies on cadmium adsorption by biochar, this biochar derived from SS gasification has a better Cd adsorption capacity. Chen et al. [36], for example, also used biochar from municipal SS and achieved Cd adsorption of up to 22.5 mg/g. Zuo et al. [42] achieved an adsorption capacity of 36.5 mg/g using SS biochar modified with $CaCO_3$ nanoparticles.

3.3.3. Chromium Removal Efficiency

The following mathematical equation, in terms of the actual factors, can be used to make predictions about Cr adsorption:

$$Y = -135.812 + 337.332A + 32.7365B - 0.14994C + 1.38881D - 48.5136AB \quad (3)$$

The normal plot of the residuals is shown in Figure 7. The residuals are normally distributed as they lie close to the straight line. The model is therefore valid.

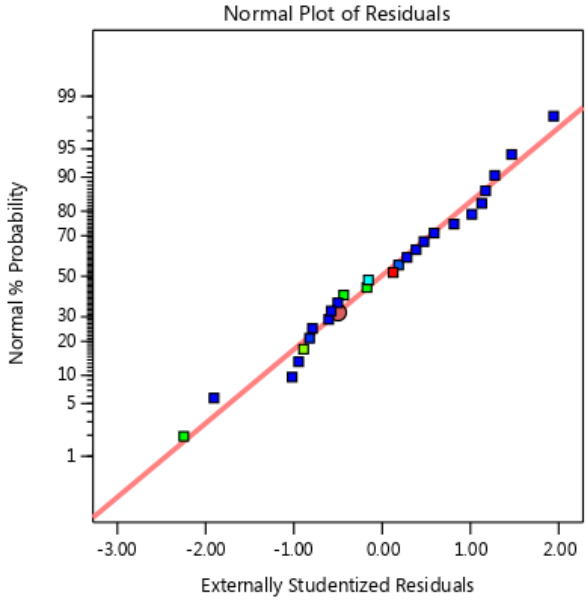

Figure 7. Normal plot of residuals for Cr removal efficiency.

The contour plot and 3D response surface for the combined effect of pH and biochar mass show their influence on Cr removal efficiency (Figure 8). As expected, a higher biochar mass leads to higher Cr adsorption. An increase in pH also has a positive effect on Cr removal efficiency. In addition, about 0.65 g of biochar is sufficient to remove 90% of Cr regardless of the pH. Liu et al. [23] obtained opposite results. The highest removal capacity of total Cr (10 mg/g) was achieved with the lowest pH (pH 2) and the lowest magnetic (nano-zero-valent iron) biochar dosage (0.5 g/L), due to the reduction of Cr(VI) to Cr(III).

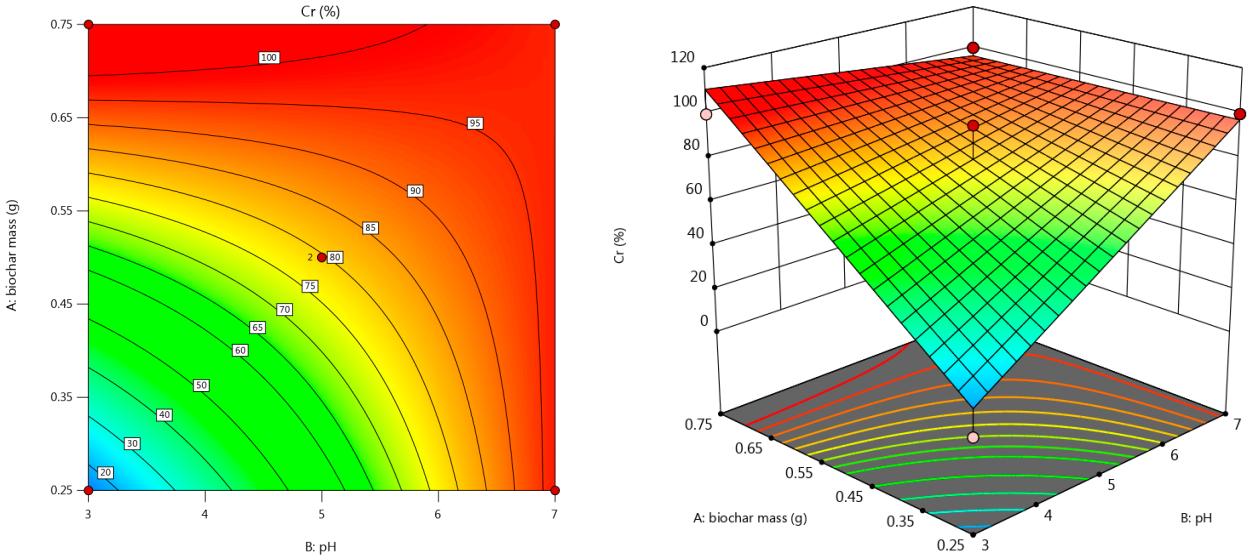

Figure 8. Contour plot (**left**) and 3D response surface (**right**) for combined effect of pH and biochar mass on Cr removal.

The perturbation plot in Figure 9 is used to compare the effects of all factors on Cr removal efficiency. Increasing the biochar mass, pH, and time has a positive effect on Cr removal efficiency. However, the removal efficiency decreases with an increase in the initial Cr concentration. In this case, Liu et al. [23] also obtained opposite results. The removal capacity of Cr increased with an increase in the initial Cr concentration. As for the reaction time, they reached equilibrium after 2 h.

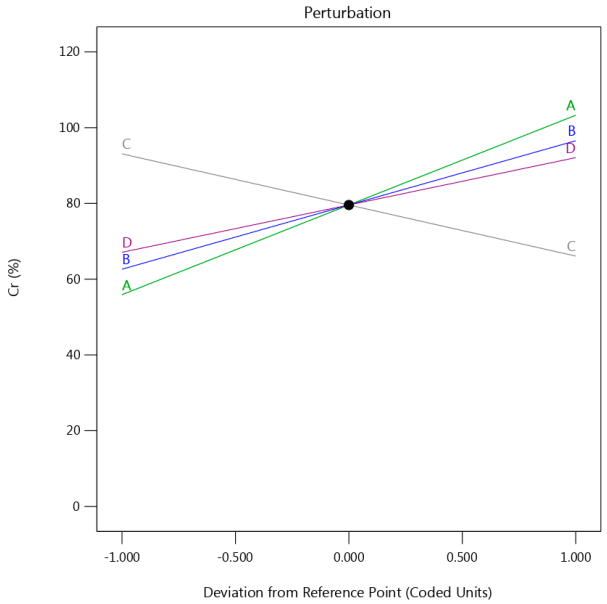

Figure 9. The perturbation plot of biochar mass (A), pH (B), initial Cr concentration (C), and time (D).

The adsorption capacity of Cr (Table 3) varies between 1.03 mg/g and 43.89 mg/g, depending on the experimental setup. For comparison, Liu et al. [23] obtained an adsorption capacity of 9.84 mg/g after 24 h.

3.3.4. Copper Removal Efficiency

For the adsorption of Cu, the following mathematical equation can be used in relation to the actual factors:

$$Y = -26.9407 + 220.803A + 20.1413B - 0.238454C - 30.4182AB \quad (4)$$

The normal plot of the residuals is shown in Figure 10. The residuals are normally distributed, and the model is valid.

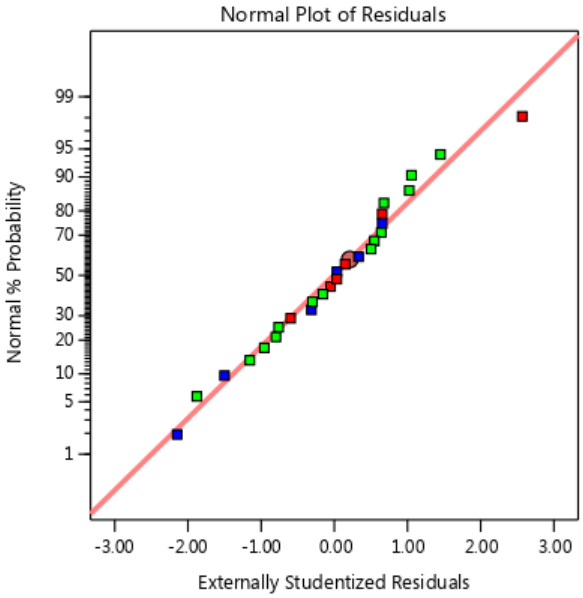

Figure 10. Normal plot of residuals for Cu removal efficiency.

The contour plot and the 3D response surface for the combined effect of pH and biochar mass show their influence on Cu removal efficiency (Figure 11). As with Cd and Cr, a higher biochar mass and a higher pH value have a positive effect on Cu adsorption. However, here too, higher efficiencies are achieved under more acidic conditions with a biochar mass of 0.65 g or more. Tang et al. [43] also found that increasing the pH promoted Cu adsorption on biochar derived from pyrolysis at 500°C, which could be due to the ion exchange effect of Ca^{2+}, Mg^{2+}, K^{+}, and Na^{+}, which are ubiquitous in municipal SS.

The perturbation plot in Figure 12 is used to compare the effects of biochar mass, pH, and initial Cu concentration on Cu removal efficiency. As with Cr, increasing the biochar mass, pH, and time positively affectes Cu removal, but the removal efficiency decreases with an increase in the initial Cu concentration.

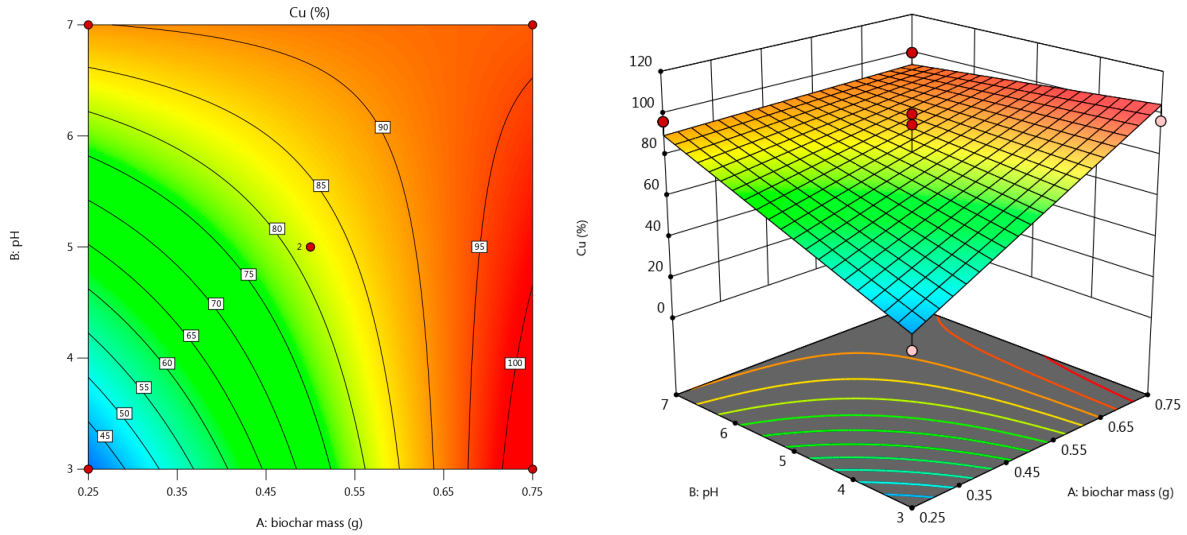

Figure 11. Contour plot (**left**) and 3D response surface (**right**) for combined effect of pH and biochar mass on Cu removal.

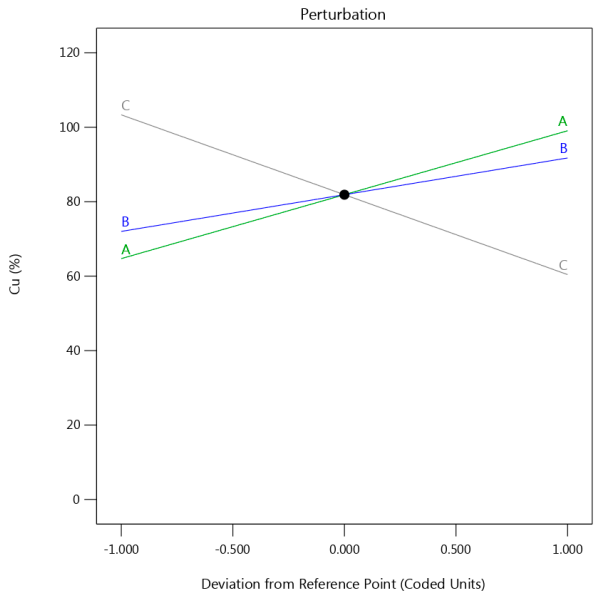

Figure 12. The perturbation plot of biochar mass (A), pH (B), and initial Cu concentration (C).

The adsorption capacity of Cu (Table 3) varies between 2.66 mg/g and 42.2 mg/g, depending on the experimental setup. Tang et al. [43] achieved an adsorption capacity of 74.51 mg/g for amino-functionalized SS biochar, which corresponds to an increase of 118% compared to experiments with biochar from pyrolysis at 500°C.

3.3.5. Lead Removal Efficiency

For Pb adsorption, the following mathematical equation can be used in terms of the actual factors:

$$Y = -118.312 - 19.0071A - 7.83457B + 0.0505995C + 0.138833AC + 0.721014B^2 - 0.00041028C^2 \quad (5)$$

The normal plot of the residuals is shown in Figure 13. The residuals are normally distributed, and the model is valid.

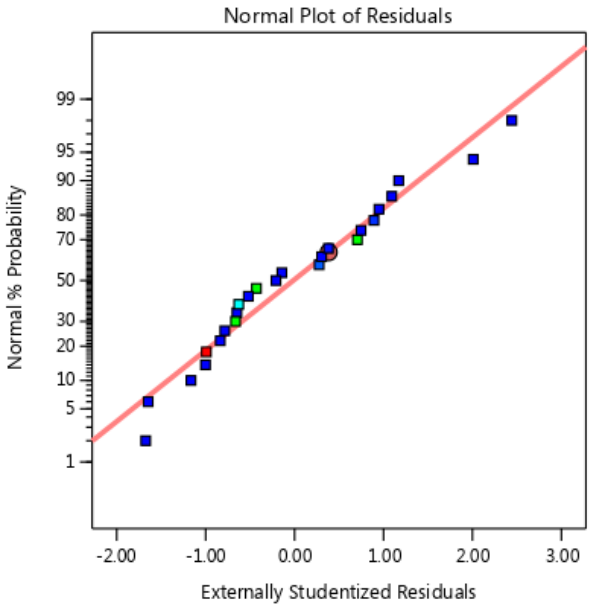

Figure 13. Normal plot of residuals for Pb removal efficiency.

The contour plot and 3D response surface for the combined effect of initial Pb concentration and biochar mass show their influence on Pb removal efficiency (Figure 14). The highest removal efficiency is achieved for an initial Pb concentration of between about 110 and 140 mg/l.

It was also found that an increase in biochar mass had no significant effect on Pb adsorption due to the saturation of the biochar. This can also be seen in the perturbation plot (Figure 15). This differs from the other heavy metals. This is also noted in the ANOVA table (Table 4), where the *p*-value of factor A—biochar mass—is 0.3615, which is above the standard value of 0.1. Factor A, which independently does not affect the Pb removal process and should be eliminated by reducing the model, is still included due to the retention of the AC ratio. Therefore, although the mass of the biochar alone does not significantly contribute to Pb removal, it does influence Pb removal in combination with the initial concentration (factor C). The same can be seen from the *p*-value, which is 0.0724 for the combination of the factors AC. Zhou et al. [44] also obtained similar results with biochar derived from banana peels. The adsorption capacities of Pb gradually decreased with an increase in the sorbent dosage, and equilibrium was reached after adding 0.05 g of adsorbent.

Pb adsorption increases as the initial Pb concentration increases, but slows down when the initial Pb concentration increases above 120 mg/L. The reason for this is that the adsorption capacity of a small mass of biochar (less than 0.55 g) is not sufficient to remove high Pb concentrations. If the mass of the biochar is 0.55 g or more, higher Pb concentrations can be removed.

Pb was not investigated in alkaline environments, as Pb ions start to precipitate at a pH above 7 [44]. In terms of the pH, 95% to 100% of Pb removal was achieved at all three pH values investigated. The highest Pb adsorption was achieved at pH 3, as lead is more soluble in an acidic environment.

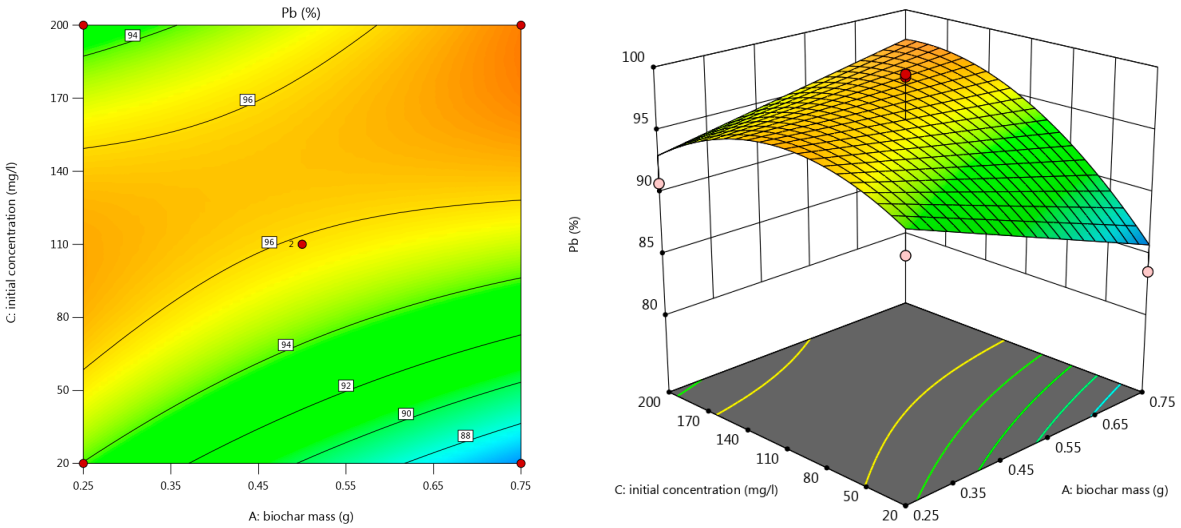

Figure 14. Contour plot (**left**) and 3D response surface (**right**) for combined effect of initial Pb concentration and biochar mass on Pb removal.

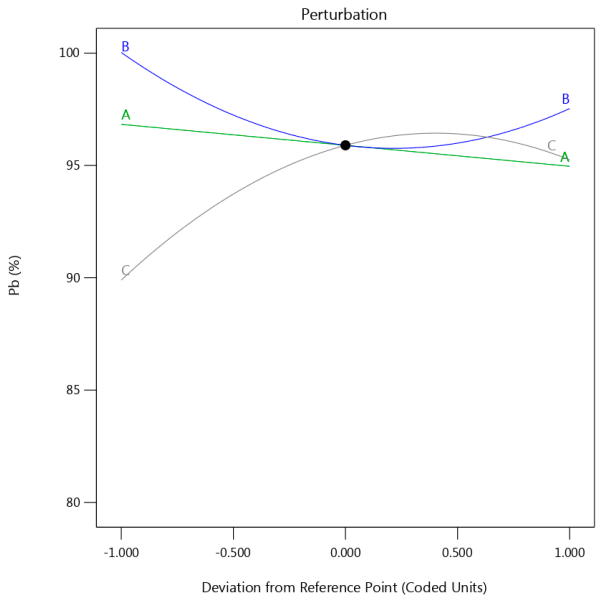

Figure 15. The perturbation plot of biochar mass (A), pH (B), and initial Pb concentration (C).

The adsorption capacity of Pb (Table 3) varies between 2.23 mg/g and 72.66 mg/g, depending on the experimental setup. For comparison, Zhang et al. [45] achieved an adsorption capacity of 22.4 mg/g, 47.59 mg/g, and 57.48 mg/g for various sludge-based biochars activated with CO_2, KOH, and CH_3COOK, respectively.

3.3.6. Optimization and Validation of the Model

The optimization tool was used to determine the factor combination that would achieve the highest removal efficiency for all four heavy metals. The aim was to maximize the efficiency of heavy metal removal while reducing the treatment time. The other parameters were kept within the ranges listed in Table 2.

Under these conditions, the model provided 81 potential solutions, of which the one with the highest attractiveness was selected for verification. The conditions for this variant were a biochar mass of 0.67 g, a pH of 3, an initial concentration of 84.40 mg/L for all four heavy metals, and a treatment time of 6 h. The expected Cd, Cr, Cu, and Pb removal

efficiencies were 99.99%, 87.35%, 100%, and 97.72%, respectively. The prediction interval (allowable deviation) for these values was 5%.

A confirmation test was carried out under the above conditions, and the removal efficiencies of Cd, Cr, Cu, and Pb obtained were 99.51%, 92.08%, 98.44%, and 97.42%, respectively. These results are within the prediction interval. It can be concluded that RSM can be effectively used to determine the operating parameters that influence the adsorption of heavy metals on biochar.

3.4. Adsorption Kinetics and Isotherms

Understanding the kinetics of heavy metal adsorption onto biochar is beneficial for optimizing the contact time. Adsorption kinetics not only provide insights into the mechanisms governing the adsorption process, but also help to identify the rate-limiting steps, which are essential for scaling up the process for industrial applications. Additional batch experiments were conducted to study the kinetics of heavy metals adsorption onto biochar. A total of 20 mg/L of Pb, Cd, Cr, and Cu solutions with a pH value of 3 were prepared, and 0.5 g of biochar was added to each solution. The solutions were agitated for up to 6 h at a constant temperature of 25 °C to ensure uniform contact between the adsorbent and adsorbates, with samples taken after 0.5, 1, 2, 3, and 6 h. The time-dependent changes in the concentrations of the heavy metals were recorded, and the kinetic data were modeled to identify the best-fit kinetic model.

The adsorption kinetics were analyzed using pseudo-first-order (PFO) and pseudo-second-order (PSO) models, which are widely used to describe adsorption processes. The PFO model assumes that the rate of adsorption is directly proportional to the number of unoccupied sites, and it is expressed as

$$q_t = q_e\ (1 - \ e^{-k_1 t}) \tag{6}$$

where q_t is the amount adsorbed at time t (mg/g), q_e is the amount of adsorbate adsorbed at equilibrium (mg/g), and k_1 is the rate constant (min^{-1}) [46,47].

The PSO model assumes that chemisorption, involving electron sharing or exchange, dominates the process. It can be described by the Equation (7), in which k_2 represents the rate constant of PSO kinetics (g/mg·min). This model often provides a better fit for processes where chemical interactions between the adsorbent and adsorbate play a major role.

$$q_t = \frac{k_2 q_e^2 t}{1 + \ k_2 q_e t} \tag{7}$$

The kinetic parameters obtained for the PFO and PSO models are presented in Table 5, and a graphical comparison is shown in Figure 16. The PSO model yields higher R^2 values (0.981–0.999) across all the metals, indicating a superior fit compared to the PFO model. Additionally, the equilibrium adsorption capacities calculated using the PSO model are closer to the experimentally observed values, suggesting that the adsorption process is likely controlled by chemisorption mechanisms. The superior fit of the PSO kinetic model in this study aligns with numerous findings in the literature. For instance, in a study by Shafiq et al. [48], the adsorption of Ni and Pb onto derived biochar showed a very good fit with the PSO kinetic model. Similarly, Mahmood-ul-Hassan et al. [49] found that Pb, Cr, and Cd adsorption on sawdust also follows the PSO model. Furthermore, similar trends for Ni and Cu adsorption on biochar were confirmed by Zhou et al. [50]. Goswami et al. [51] also described Cd adsorption onto biochar using the PSO model. Collectively, these studies corroborate the results of this work, reinforcing the conclusion that the PSO model is more appropriate for describing heavy metal adsorption onto biochar.

The adsorption of heavy metals onto biochar likely involves chemisorption, as suggested by the PSO kinetics, with the potential mechanisms including surface complexation.

Table 5. Calculated parameters for tested kinetic models.

	PSO					PFO			
	Pb	**Cd**	**Cr**	**Cu**		**Pb**	**Cd**	**Cr**	**Cu**
q_e (mg/g)	3.008	3.019	3.018	3.028	q_e (mg/g)	1.573	1.973	2.273	2.461
k_2 (g/mg·h)	5.212	2.533	0.681	1.077	k_1 (h^{-1})	1.689	1.732	0.604	0.989
R^2	0.999	0.997	0.981	0.993	R^2	0.922	0.918	0.916	0.984

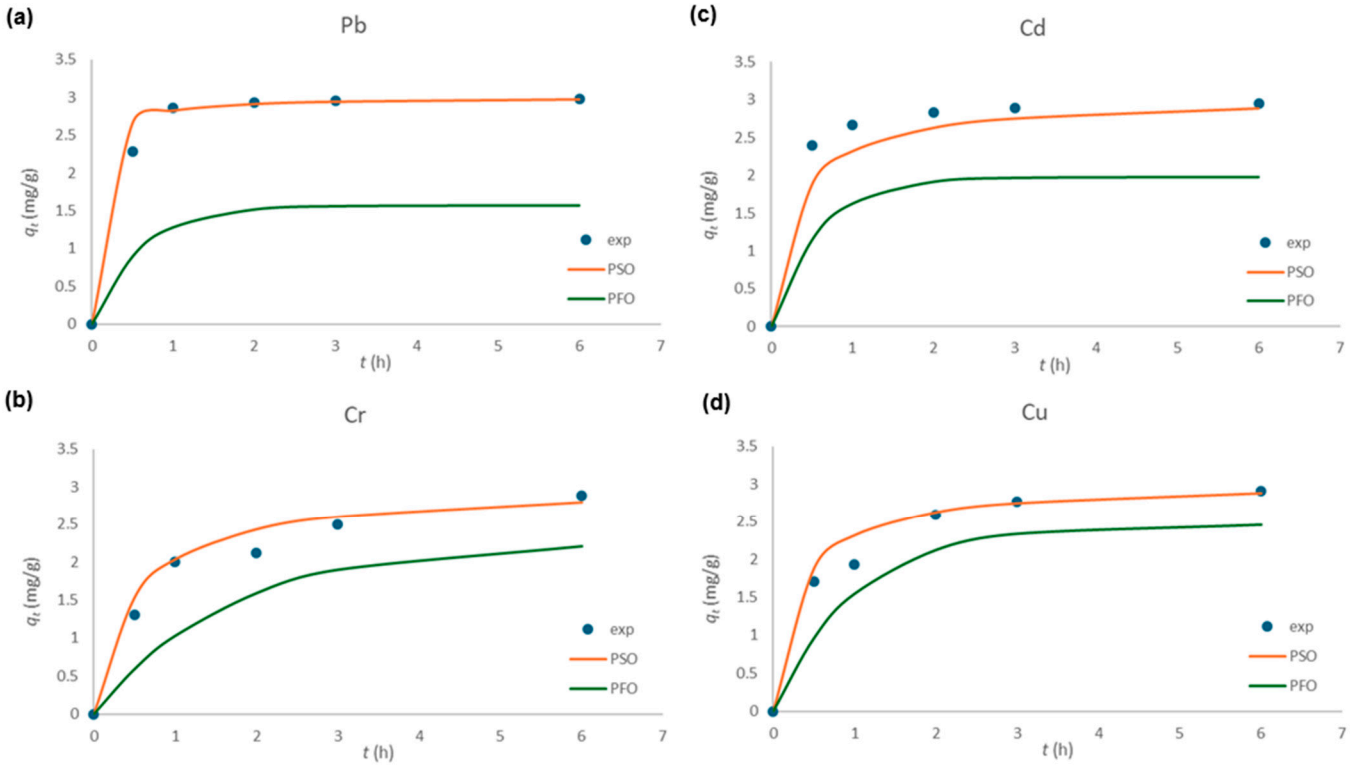

Figure 16. The comparison of PSO and PFO kinetic models for (**a**) Pb, (**b**) Cr, (**c**) Cd, and (**d**) Cu removal.

Adsorption isotherms help to understand the interaction between the adsorbate and the adsorbent surface, providing insights into the adsorption capacity and mechanism [52]. In this study, two widely used models, the Langmuir and Freundlich isotherms, are applied to describe the equilibrium adsorption of Pb, Cd, Cr, and Cu on biochar. Adsorption isotherms are crucial for understanding how heavy metals are retained by biochar at various concentrations.

The Langmuir isotherm, which assumes monolayer adsorption onto a surface with a finite number of identical sites, is expressed as

$$q_e = \frac{q_m k_l c_e}{1 + k_l c_l} \quad (8)$$

where q_m is the maximum adsorption capacity, c_e is the equilibrium concentration, and k_l is the Langmuir constant [46,53]. The Freundlich isotherm describes adsorption on heterogeneous surfaces, suggesting multilayer adsorption, and is given by Equation (9):

$$q_e = k_f c_e^{\frac{1}{n}} \quad (9)$$

where k_f and n are empirical constants related to the adsorption capacity and intensity [46,53].

The adsorption experiments used for the isotherm studies were conducted using 0.5 g of biochar at a room temperature of 25 °C, with an equilibrium time of 6 h, pH value of 3, and initial metal concentrations of 10, 110, and 200 mg/L. Both Freundlich and Langmuir isotherms were evaluated to analyze the interaction between the heavy metal ions and the biochar surface. As listed in Table 6, the Freundlich model exhibits higher R^2 values for most metals, except for Cd, where the Langmuir model performs equally well. This suggests that the adsorption of Pb, Cr, and Cu onto biochar occurs predominantly on heterogeneous surfaces, supporting a multilayer adsorption mechanism. Interestingly, the Langmuir model shows excellent agreement for Cd adsorption, suggesting that Cd ions may form a uniform monolayer on the biochar surface. Figure 17 compares both models for the adsorption of Cu, which can be described by either one. It is important to note that the isotherms obtained in this study are based on limited experimental data and do not include enough points to be considered fully representative of equilibrium conditions. However, the presented results still provide indicative trends of the adsorption process.

Table 6. Langmuir and Freundlich isotherm parameters.

	Langmuir					**Freundlich**			
	Pb	**Cd**	**Cr**	**Cu**		**Pb**	**Cd**	**Cr**	**Cu**
q_m	39.996	26.042	18.018	17.986	n	1.570	2.285	2.861	2.766
k_l	0.594	0.492	0.074	0.146	k_f	12.622	6.448	3.195	3.542
R^2	0.773	0.997	0.864	0.988	R^2	0.990	0.865	0.975	0.997

The results of this study align well with the findings of others, such as Ye et al. [54], where the maximum adsorption capacity for Pb was 40.8 mg/g and for Cd it was 24.2 mg/g. Shafiq et al. [48] also found that Pb ions are more quickly absorbed on biochar and have a higher maximum capacity. Although studies, such as those of Ye at al. [54], Shafiq et al. [48] and Zou et al. [50], have found that the Langmuir model better describes the adsorption of heavy metals onto various biochars, other authors, such as Khudair et al. [55] and Reddy et al. [56], have concluded that the Langmuir model is a better fit. Similarly to results of this study, Zhou et al. [44] concluded that both models can show a very good fit, depending on the heavy metal.

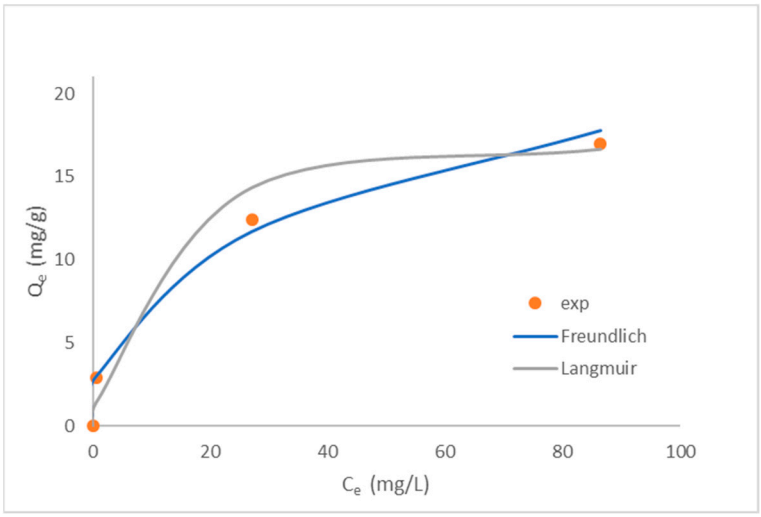

Figure 17. Comparison of Freundlich and Langmuir isotherms for copper.

4. Discussion

The presented technique for heavy metals removal from wastewater offers many advantages, including low cost, high selectivity, efficient removal even at low concentrations, ease of use, simple design, high capacity, and minimal by-product generation, consistent with the findings from previous studies [19]. However, the novel biochar derived from the experimental gasification plant used in this study offers additional environmental and economic benefits. Due to its high carbon content, the presence of metal oxides (Ca, Al, Fe, and Mg) on the surface, and its highly porous structure, this biochar demonstrated exceptional efficiency at removing selected heavy metals. The adsorption capacities of the pristine biochar (without any modifications) were generally comparable to, and in some cases even exceeded, those reported in previous studies where modified biochars were predominantly used [3,14]. Xu et al. [57] reported similar carbon contents (50–60%) in SS-derived biochar, but with considerably lower levels of the major metal oxides (Si, Ca, Fe, and Al).

Fan et al. [58] reported a maximum adsorption capacity of 38.49 mg/g for Cu(II) using $Na_4P_2O_7$-modified SS biochar at 35 °C. Shah et al. [13] found that the optimal contact times for removing Zn^{2+} and Cd^{2+} were 80 and 140 min, achieving removal rates of 95.51% and 97.54%, respectively, from 50 mg/L spiked solutions using 25 g/l biochar. The optimum pH was 8–9 at 40 °C, suggesting some metal ion precipitation in alkaline conditions. Maximum adsorption capacities were 3.02 mg/g for Cd^{2+} and 2.51 mg/g for Zn^{2+}, comparable to other adsorbents. Isotherm studies confirmed that the Langmuir model fit well, with R^2 values of 0.9846 and 0.9816 for Cd^{2+} and Zn^{2+}. However, the overall results of the removal efficiency still fall short when compared to those achieved in this study.

The surface of biochar carries a negative charge due to the presence of specific functional groups. As a result, positively charged metals are retained on the surface through electrostatic interactions [59]. The ion exchange process between the adsorbent (SS biochar) and the treated metals occurs as a result of the dissociation of acidic or ionic groups present in the biochar [13].

Kang et al. [22] found that Cr(VI) removal involved electrostatic attraction, reduction, and complexation precipitation by surface functional groups. Cu(II) removal occurred through surface adsorption, complexation precipitation, and reduction by Fe when nano-zero-valent iron-modified SS biochar was used. For both metals, the pseudo-second-order model showed a better correlation than the pseudo-first-order model, indicating that adsorption was primarily chemical, involving surface complexation rather than simple physical adsorption. These authors concluded that the Langmuir model better explained the adsorption of Cr(VI) and Cu(II) by both modified and unmodified biochar compared to the Freundlich model. Their findings were consistent with those of Yan et al. [60], which suggested that Cu(II) and Cr(VI) form a single-layer coverage on heterogeneous biochar surfaces. A mixed-fit scenario (Langmuir for some metals, Freundlich for others), noted in this study, is common for systems involving heterogeneous adsorbents like biochar. The superior performance of the Freundlich model for most metals, particularly Pb, Cr, and Cu, highlights the importance of heterogeneity in biochar's adsorption mechanism. The strong fit of the Langmuir model for Cd, on the other hand, suggests that biochar modification could optimize uniform adsorption for specific metals. These findings emphasize the versatility of biochar as an adsorbent in multicomponent systems. Cao et al. [14] concluded that the adsorption process of heavy metal ions by biochar included several mechanisms: physical adsorption, electrostatic attraction, surface microprecipitation, surface complexation, ion exchange, and co-precipitation.

The solution pH is a key factor in metal adsorption, affecting electrostatic interactions, ion exchange, and metal speciation [41]. The authors Shah et al. [13] conducted desorption of biochar, saturated with heavy metals, using a 1 M HCl solution until

equilibrium was reached. In the first cycle, the removal was 94.5% for Cd^{2+} and 78% for Zn^{2+}, but in the second and third cycles, the removal dropped to 30% and 15% for Cd^{2+} and 70% and 16% for Zn^{2+}. To improve performance, the authors adjusted the pH of the solution to 7.0 in cycles 4, 5, and 6, leading to the optimal removal of 99.5% for Cd^{2+} and 84.5% for Zn^{2+}.

Cao et al. [14], based on a comprehensive literature review, highlighted the importance of integrating pretreatments and post-treatments with biochar preparation (its modification) to enhance the adsorption capacity of pristine biochar, while also addressing the issue of avoiding toxic compound contamination during environmental remediation. One of the primary challenges in using SS-derived biochar for environmental improvement is the formation of toxic compounds. The presence of pollutants and toxic substances in biochar, including volatile organic compounds, heavy metals, potentially toxic elements, environmentally persistent free radicals, polycyclic aromatic hydrocarbons, and dioxins, depends on the raw SS source and the conditions of the thermal treatments [45]. However, these challenges have mostly been overcome by using the novel biochar presented in this research. Since biochar is a byproduct of SS processing, it has no material value and only requires proper disposal. The primary aim was to maximize heavy metals removal efficiency without focusing on minimizing the biochar quantity used. Given the abundance and anticipated low cost of SS biochar, its practical applications appear promising.

Before the commercialization of biosorbents, proper attention must be given to their final disposal. Few studies on biochar have focused on the regeneration and reuse of spent adsorbents, often overlooking their final disposal. Disposing of spent biomaterials contaminated with hazardous organic ions presents significant challenges, with most solutions relying on incineration or landfill disposal. Biochar containing heavy metals can be disposed of after metal recovery or immediately post-adsorption. In both cases, there is a risk of secondary pollution from the biochar and chemicals used. Biochar loaded with heavy metals can harm the environment and human health, making it crucial to ensure the complete recovery of heavy metals before release into the environment [14]. The authors of this paper propose the further use of the spent biochar in the construction materials industry based on previous technical and ecological studies that have already explored its use as a substitute for parts of the raw materials in concrete [28] and brick products [29]. Future research should investigate the use of biochar, previously used as an adsorbent in wastewater treatment, in the production of different construction materials. Significant differences in the technical properties of the resulting materials are not expected, but their ecological safety (considering that biochar has absorbed additional pollutants) must be thoroughly re-evaluated. However, an encouraging fact is that cement and clay-based materials have the ability to incorporate potentially harmful substances into the hardened matrix of the final products during the curing process.

Although this paper initially analyzed wide ranges of initial concentrations for each heavy metal, which realistically represent extremely high concentration values of these pollutants potentially present in real wastewater, the intention was to cover a broad spectrum of boundary conditions. Since adsorbents should also be effective at lower pollutant concentrations, further research should aim to conduct experiments at lower, more realistic concentrations. Future research should also explore the removal of these and other heavy metals from real wastewater samples to assess how co-existing ions affect adsorption under typical conditions. The economic feasibility and cost-effectiveness of biochar should also be assessed.

5. Conclusions

Managing the growing global production of SS and removing toxic heavy metals from water are environmental challenges of increasing interest. Biochar, a cost-effective adsorbent, has previously demonstrated an adsorption performance at least comparable to traditional materials. While most research has focused on chemically or physically modified biochar for enhanced adsorption, this study highlighted the potential of pristine biochar produced through the thermal gasification of SS in an experimental plant, demonstrating its high efficiency at removing Cd, Cr, Cu, and Pb from synthetic wastewater. Its adsorption capacity reached up to 46.64 mg/g for Cd, 43.89 mg/g for Cr, 42.42 mg/g for Cu, and 72.66 mg/g for Pb from single-component synthetic solutions in acidic-to-neutral conditions, achieving removal efficiencies of over 99% under optimal conditions.

A total of 104 experiments were conducted to analyze the influence of biochar mass, initial heavy metal concentration, pH, and time on removal efficiency. While all the parameters affected Cd and Cr removal, the initial metal concentration had the greatest impact on Cu and Pb removal. The process optimization showed that under the following conditions—0.67 g biochar, pH 3, 84.40 mg/L initial concentration, and 6 h treatment—the removal efficiencies were 99.51% for Cd, 92.08% for Cr, 98.44% for Cu, and 97.42% for Pb.

The adsorption followed PSO kinetics, with Cd aligning with the Langmuir model and Pb, Cr, and Cu adhering to the Freundlich model. This demonstrates biochar's adaptability as an adsorbent, offering both heterogeneous adsorption for most metals and uniform adsorption for Cd.

Using unmodified biochar offers simplicity, cost-effectiveness, and reduced environmental impact while maintaining adsorption efficiency, suggesting its potential as a promising adsorbent for wastewater treatment.

Considering the results of previous studies where the same biochar was used as a partial replacement for raw materials in the production of construction materials, such as concrete and bricks, further research should explore the feasibility of using biochar as an adsorbent in wastewater treatment over multiple cycles and, once its maximum adsorption capacity is reached, the possibility of reusing it as a partial substitute for raw materials in the construction industry. This approach would offer a new, sustainable, and eco-friendly strategy for the comprehensive utilization of waste materials. Future studies should focus on testing these applications, including experiments with real wastewater, evaluating performance across multiple adsorption–desorption cycles, and assessing the economic feasibility and cost-effectiveness to support the practical use of biochar.

Author Contributions: Conceptualization, D.N. and H.P.; methodology, D.N. and K.L.; software, H.P. and K.L.; validation, D.N., H.P. and K.L.; formal analysis, K.L.; investigation, D.N. and H.P.; resources, D.N. and D.V.; data curation, H.P. and K.L.; writing—original draft preparation, D.N., H.P. and K.L.; writing—review and editing, D.N. and D.V.; visualization, H.P.; supervision, D.N.; project administration, K.L.; funding acquisition, D.V. and D.N. All authors have read and agreed to the published version of the manuscript.

Funding: This research was funded by the Croatian Science Foundation under project "UIP-2020-02-1160—Purification of Microbiologically and Chemically Contaminated Drinking Water by Electrochemical and Ultrasonic Processes".

Institutional Review Board Statement: Not applicable.

Informed Consent Statement: Not applicable.

Data Availability Statement: All the main processed data are contained within this article. The remaining raw datasets from the conducted tests are available upon request to the authors.

Acknowledgments: This work was fully supported by the Croatian Science Foundation under project "UIP-2020-02-1160—Purification of Microbiologically and Chemically Contaminated Drinking Water by Electrochemical and Ultrasonic Processes".

Conflicts of Interest: The authors declare no conflicts of interest.

References

1. Di Giacomo, G.; Romano, P. Evolution and Prospects in Managing Sewage Sludge Resulting from Municipal Wastewater Purification. *Energies* **2022**, *15*, 5633. https://doi.org/10.3390/en15155633.
2. Feng, J.; Burke, I.T.; Chen, X. Assessing metal contamination and speciation in sewage sludge: Implications for soil application and environmental risk. *Rev. Environ. Sci. Biotechnol*. **2023**, *22*, 1037–1058. https://doi.org/10.1007/s11157-023-09675-y.
3. Zhao, L.; Sun, Z.-F.; Pan, X.-W.; Tan, J.-Y.; Yang, S.-S.; Wu, J.-T.; Chen, C.; Yuan, Y.; Ren, N.-Q. Sewage sludge derived biochar for environmental improvement: Advances, challenges, and solutions. *Water Res. X* **2023**, *18*, 100167. https://doi.org/10.1016/j.wroa.2023.100167.
4. Agrafioti, E.; Bouras, G.; Kalderis, D.; Diamadopoulos, E. Biochar production by sewage sludge pyrolysis. *J. Anal. Appl. Pyrolysis* **2013**, *101*, 72–78. https://doi.org/10.1016/j.jaap.2013.02.010.
5. Rangabhashiyam, S.; dos Santos Lins, P.V.; de Magalhães Oliveira, L.M.T.; Sepulveda, P.; Ighalo, J.O.; Rajapaksha, A.U.; Meili, L. Sewage sludge-derived biochar for the adsorptive removal of wastewater pollutants: A critical review. *Environ. Pollut.* **2022**, *293*, 118581. https://doi.org/10.1016/j.envpol.2021.118581.
6. Wang, X.; Chang, V.W.-C.; Li, Z.; Chen, Z.; Wang, Y. Co-pyrolysis of sewage sludge and organic fractions of municipal solid waste: Synergistic effects on biochar properties and the environmental risk of heavy metals. *J. Hazard. Mater.* **2021**, *412*, 125200. https://doi.org/10.1016/j.jhazmat.2021.125200.
7. Zhou, D.; Liu, D.; Gao, F.; Li, M.; Luo, X. Effects of Biochar-Derived Sewage Sludge on Heavy Metal Adsorption and Immobilization in Soils. *Int. J. Environ. Res. Public Health* **2017**, *4*, 681. https://doi.org/10.3390/ijerph14070681.
8. Ramachandran, S.; Yao, Z.; You, S.; Massier, T.; Stimming, U.; Wang, C.-H. Life cycle assessment of a sewage sludge and woody biomass co-gasification system. *Energy* **2017**, *137*, 369–376. https://doi.org/10.1016/j.energy.2017.04.139.
9. Kang, B.S.; Farooq, A.; Valizadeh, B.; Lee, D.; Seo, M.W.; Jung, S.-C.; Hussain, M.; Kim, Y.M.; Khan, M.A.; Jeon, B.-H.; et al. Valorization of sewage sludge via air/steam gasification using activated carbon and biochar as catalysts. *Int. J. Hydrogen Energy* **2024**, *54*, 284–293. https://doi.org/10.1016/j.ijhydene.2023.04.188.
10. Chen, X.; Chen, G.; Chen, L.; Chen, Y.; Lehmann, J.; McBride, M.B.; Hay, A.G. Adsorption of copper and zinc by biochars produced from pyrolysis of hardwood and corn straw in aqueous solution. *Bioresour. Technol.* **2011**, *102*, 19, 8877–8884. https://doi.org/10.1016/j.biortech.2011.06.078.
11. Oliveira, F.R.; Patel, A.K.; Jaisi, D.P.; Adhikari, S.; Lu, H.; Khanal, S.K. Environmental application of biochar: Current status and perspectives. *Bioresour. Technol.* **2017**, *246*, 110–122. https://doi.org/10.1016/j.biortech.2017.08.122.
12. Xiang, W.; Zhang, X.; Chen, J.; Zou, W.; He, F.; Hu, X.; Tsang, D.C.W.; Ok, Y.S.; Gao, B. Biochar technology in wastewater treatment: A critical review. *Chemosphere* **2020**, *252*, 126539. https://doi.org/10.1016/j.chemosphere.2020.126539.
13. Shah, A.; Zakharova, J.; Batool, M.; Coley, M.P.; Arjunan, A.; Hawkins, A.J.; Bolarinwa, T.; Devi, S.; Thumma, A.; Williams, C. Removal of cadmium and zinc from water using sewage sludge-derived biochar. *Sustain. Chem. Environ.* **2024**, *6*, 100118. https://doi.org/10.1016/j.scenv.2024.100118.
14. Cao, J.; Jiang, Y.; Tan, X.; Li, L.; Cao, S.; Dou, J.; Chen, R.; Hu, X.; Qiu, Z.; Li, M.; et al. Sludge-based biochar preparation: Pyrolysis and co-pyrolysis methods, improvements, and environmental applications. *Fuel* **2024**, *373*, 132265. https://doi.org/10.1016/j.fuel.2024.132265.
15. Ahmad, M.; Rajapaksha, A.U.; Lim, J.E.; Zhang, M.; Bolan, N.; Mohan, D.; Vithanage, M.; Lee, S.S.; Ok, Y.S. Biochar as a sorbent for contaminant management in soil and water: A review. *Chemosphere* **2014**, *99*, 19–33. https://doi.org/10.1016/j.chemosphere.2013.10.071.
16. Singh, S.; Kumar, V.; Singh Dhanjal, D.; Datta, S.; Bhatia, D.; Dhiman, J.; Samuel, J.; Prasad, R.; Singh, J. A sustainable paradigm of sewage sludge biochar: Valorization, opportunities, challenges and future prospects. *J. Clean. Prod.* **2020**, *269*, 122259. https://doi.org/10.1016/j.jclepro.2020.122259.
17. Rozada, F.; Otero, M.; Moran, A.; Garcia, A.I. Adsorption of heavy metals onto sewage sludge-derived materials. *Bioresour. Technol.* **2008**, *99*, 6322–6338. https://doi.org/10.1016/j.biortech.2007.12.015.

18. Yin, Q.; Liu, M.; Ren, H. Biochar produced from the co-pyrolysis of sewage sludge and walnut shell for ammonium and phosphate adsorption from water. *J. Environ. Manag.* **2019**, *249*, 109410. https://doi.org/10.1016/j.jenvman.2019.109410.
19. Usman, M.O.; Aturagaba, G.; Ntale, M.; Nyakairu, G.W. A review of adsorption techniques for removal of phosphates from wastewater, *Water Sci. Technol.* **2022**, *86*, 3113–3132. https://doi.org/10.2166/wst.2022.382.
20. Wu, X.; Quan, W.; Chen, Q.; Gong, W.; Wang, A. Efficient Adsorption of Nitrogen and Phosphorus in Wastewater by Biochar, *Molecules* **2024**, *29*, 1005. https://doi.org/10.3390/molecules29051005.
21. Lin, Q.H.; Cheng, H.; Chen, G.Y. Preparation and characterization of carbonaceous adsorbents from sewage sludge using a pilot-scale microwave heating equipment, *J. Anal. Appl. Pyrol.* **2012**, *93*, 113–119. https://doi.org/10.1016/j.jaap.2011.10.006.
22. Kang, X.; Xiao, F.; Zhou, S.; Zhang, Q.; Qiu, L.; Wang, L. Study on the performance of sewage sludge biochar modified by nZVI to remove Cu(II) and Cr(VI) in water. *Water Sci. Technol.* **2022**, *86*, 1821–1834. https://doi.org/10.2166/wst.2022.302.
23. Liu, L.; Liu, X.; Wang, D.; Lin, H.; Huang, L. Removal and reduction of Cr(VI) in simulated wastewater using magnetic biochar prepared by co-pyrolysis of nano-zerovalent iron and sewage sludge. *J. Clean. Prod.* **2020**, *257*, 120562. https://doi.org/10.1016/j.jclepro.2020.120562.
24. Wang, Z.; Shen, R.; Ji, S.; Xie, L.; Zhang, H. Effects of biochar derived from sewage sludge and sewage sludge/cotton stalks on the immobilization and phytoavailability of Pb, Cu, and Zn in sandy loam soil. *J. Hazard. Mater.* **2021**, *419*, 126468. https://doi.org/10.1016/j.jhazmat.2021.126468.
25. Zhang, X.; Zhao, B.; Liu, H.; Zhao, Y.; Li, L. Effects of pyrolysis temperature on biochar's characteristics and speciation and environmental risks of heavy metals in sewage sludge biochars. *Environ. Technol. Innov.* **2022**, *26*, 102288. https://doi.org/10.1016/j.eti.2022.102288.
26. Zhu, Y.; Wei, J.; Li, J. Decontamination of Cr(VI) from water using sewage sludge derived biochar: Role of environmentally persistent free radicals. *Chin. J. Chem. Eng.* **2022**, *56*, 97–103. https://doi.org/10.1016/j.cjche.2022.06.015.
27. Li, J.; Cao, L.; Li, B.; Huang, H.; Yu, W.; Sun, C.; Long, K.; Young, B. Utilization of activated sludge and shell wastes for the preparation of Ca-loaded biochar for phosphate removal and recovery. *J. Clean. Prod.* **2023**, *382*, 135395. https://doi.org/10.1016/j.jclepro.2022.135395.
28. Nakić, D.; Vouk, D.; Štirmer, N.; Serdar, M. Management of sewage sludge—New possibilities involving partial cement replacement. *Civ. Eng.* **2018**, *70*, 277–286. https://doi.org/10.14256/JCE.2164.2017.
29. Bubalo, A.; Vouk, D.; Ćurković, L.; Rogošić, M.; Nakić, D.; Cheeseman, C. Influence of combustion temperature on the performance of sewage sludge ash as a supplementary material in manufacturing bricks. *Constr. Build. Mater.* **2023**, *404*, 133126. https://doi.org/10.1016/j.conbuildmat.2023.133126.
30. López, R.; Antelo, J.; Fiol, S.; Macías-García, F. Phosphate adsorption on an industrial residue and subsequent use as an amendment for phosphorous deficient soils. *J. Clean. Prod.* **2019**, *230*, 844–853. https://doi.org/10.1016/j.jclepro.2019.05.092.
31. Nardis, B.O.; Santana Da Silva Carneiro, J.; Souza, I.M.G.D.; Barros, R.G.D.; Azevedo Melo, L.C. Phosphorus recovery using magnesium-enriched biochar and its potential use as fertilizer. *Arch. Agron. Soil Sci.* **2020**, *67*, 1017–1033. https://doi.org/10.1080/03650340.2020.1771699.
32. Yao, Y.; Gao, B.; Chen, J.J.; Zhang, M.; Inyang, M.; Li, Y.C.; Alva, A.; Yang, L.Y. Engineered carbon (biochar) prepared by direct pyrolysis of Mg-accumulated tomato tissues: Characterization and phosphate removal potential. *Bioresour. Technol.* **2013**, *138*, 8–13. https://doi.org/10.1016/j.biortech.2013.03.057.
33. Bubalo, A.; Vouk, D.; Maljković, D.; Bolanča, T. Gasification of Sewage Sludge in a Rotary Kiln Reactor—A Case Study with Incorporation of Sewage Sludge Ash in Brick Production. *Chem. Biochem. Eng. Q.* **2022**, *36*, 77–87. https://doi.org/10.15255/cabeq.2021.2030.
34. Nakić, D.; Vouk, D.; Donatello, S.; Anić Vučinić, A. Environmental impact of sewage sludge ash assessed through leaching. *Eng. Rev.* **2017**, *37*, 222–234.
35. Hu, H.Y.; Liu, H.; Shen, W.Q.; Luo, G.Q.; Li, A.J.; Lu, Z.L.; Yao, H. Comparison of CaO's effect on the fate of heavy metals during thermal treatment of two typical types of MSWI fly ashes in China. *Chemosphere* **2013**, *93*, 590–596. https://doi.org/10.1016/j.chemosphere.2013.05.077.
36. Chen, T.; Zhang, Y.; Wang, H.; Lu, W.; Zhou, Z.; Zhang, Y.; Ren, L. Influence of pyrolysis temperature on characteristics and heavy metal adsorptive performance of biochar derived from municipal sewage sludge. *Bioresour. Technol.* **2014**, *164*, 47–54. https://doi.org/10.1016/j.biortech.2014.04.048.
37. Zielinska, A.; Oleszczuk, P.; Charmas, B.; Skubiszewska-Zieba, J.; Pasieczna-Patkowska, S. Effect of sewage sludge properties on the biochar characteristic. *J. Anal. Appl. Pyrolysis* **2015**, *112*, 201–213. https://doi.org/10.1016/j.jaap.2015.01.025.

38. Kończak, M.; Oleszczuk, P. Co-pyrolysis of sewage sludge and biomass in carbon dioxide as a carrier gas affects the total and leachable metals in biochars. *J. Hazard. Mater.* **2020**, *400*, 123144. https://doi.org/10.1016/j.jhazmat.2020.123144.
39. Li, J.; Li, L.; Suvarna, M.; Pan, L.; Tabatabaei, M.; Sik Ok, Y.; Wang, X. Wet wastes to bioenergy and biochar: A critical review with future perspectives. *Sci. Total Environ.* **2022**, *817*, 152921. https://doi.org/10.1016/j.scitotenv.2022.152921.
40. Anderson, M.J.; Whitcomb, P.J. *DOE Simplified: Practical Tools for Effective Experimentation*; Taylor & Francis Group: Boca Raton, FL, USA, 2007; 268p.
41. Chen, T.; Zhou, Z.; Han, R.; Meng, R.; Wang, H.; Lu, W. Adsorption of cadmium by biochar derived from municipal sewage sludge: Impact factors and adsorption mechanism. *Chemosphere* **2015**, *134*, 286–293. https://doi.org/10.1016/j.chemosphere.2015.04.052.
42. Zuo, W.Q.; Chen, C.; Cui, H.J.; Fu, M.L. Enhanced removal of Cd(II) from aqueous solution using $CaCO_3$ nanoparticle modified sewage sludge biochar. *RSC Adv.* **2017**, *7*, 16238–16243. https://doi.org/10.1039/c7ra00324b.
43. Tang, S.; Shao, N.; Zheng, C.; Yan, F.; Zhang, Z. Amino-functionalized sewage sludge-derived biochar as sustainable efficient adsorbent for Cu(II) removal. *Waste Manag.* **2019**, *90*, 17–28. https://doi.org/10.1016/j.wasman.2019.04.042.
44. Zhou, N.; Chen, H.; Xi, J.; Yao, D.; Zhou, Z.; Tian, Y.; Lu, X. Biochars with Excellent Pb(II) Adsorption Property Produced from Fresh and Dehydrated Banana Peels via hydrothermal Carbonization. *Bioresour. Technol.* **2017**, *232*, 204–210. https://doi.org/10.1016/j.biortech.2017.01.074.
45. Zhang, J.; Shao, J.; Jin, Q.; Li, Z.; Zhang, X.; Chen, Y.; Zhang, S.; Chen, H. Sludge-based biochar activation to enhance Pb(II) adsorption. *Fuel* **2019**, *252*, 101–108. https://doi.org/10.1016/j.fuel.2019.04.096.
46. Li, X.; Jia, H.; Jiang, L.; Mou, Z.; Zhang, B.; Zhang, Z.; Chen, Y. Biochar Prepared from Steam-Exploded Bitter Melon Vine for the Adsorption of Methylene Blue from Aqueous Solution: Kinetics, Isotherm, Thermodynamics and Mechanism. *Sustainability* **2024**, *16*, 7278. https://doi.org/10.3390/su16177278.
47. Murphy, O.P.; Vashishtha, M.; Palanisamy, P.; Kumar, K.V. A Review on the Adsorption Isotherms and Design Calculations for the Optimization of Adsorbent Mass and Contact Time. *ACS Omega* **2023**, *8*, 17407–17430. https://doi.org/10.1021/acsomega.2c08155.
48. Shafiq, M.; Alazba, A.A.; Amin, M.T. Kinetic and Isotherm Studies of Ni^{2+} and Pb^{2+} Adsorption from Synthetic Wastewater Using Eucalyptus camdulensis—Derived Biochar. *Sustainability* **2021**, *13*, 3785. https://doi.org/10.3390/su13073785.
49. Mahmood-ul-Hassan, M.; Yasin, M.; Yousra, M. Kinetics, isotherms, and thermodynamic studies of lead, chromium, and cadmium bio-adsorption from aqueous solution onto Picea smithiana sawdust. *Environ. Sci. Pollut. Res.* **2018**, *25*, 12570–12578. https://doi.org/10.1007/s11356-018-1300-3.
50. Zhou, R.; Zhang, M.; Shao, S. Optimization of target biochar for the adsorption of target heavy metal ion. *Sci. Rep.* **2022**, *12*, 13662. https://doi.org/10.1038/s41598-022-17901-w.
51. Goswami, R.; Shim, J.; Deka, S.; Kumari, D.; Kataki, R.; Kumar, M. Characterization of cadmium removal from aqueous solution by biochar produced from Ipomoea fistulosa at different pyrolytic temperatures. *Ecol. Eng.* **2016**, *97*, 444–451. https://doi.org/10.1016/j.ecoleng.2016.10.007.
52. Shi, X.; Yang, W.; Li, J.; Yao, Z. The Application of Biochar as Heavy Metals Adsorbent: The Preparation, Mechanism, and Perspectives. *Int. J. Environ. Res.* **2024**, *18*, 41. https://doi.org/10.1007/s41742-024-00592-8.
53. Doczekalska, B.; Ziemińska, N.; Kuśmierek, K.; Świątkowski, A. Activated Carbons Derived from Different Parts of Corn Plant and Their Ability to Remove Phenoxyacetic Herbicides from Polluted Water. *Sustainability* **2024**, *16*, 7341. https://doi.org/10.3390/su16177341.
54. Ye, Q.; Li, Q.; Li, X. Removal of heavy metals from wastewater using biochars: Adsorption and mechanisms. *Environ. Pollut. Bioavailab.* **2022**, *34*, 385–394. https://doi.org/10.1080/26395940.2022.2120542.
55. Khudair, D.S.; Abdulaziz, Y.I. Synthesis and Characterization of Novel Biochar Developed from Peganum Harmala Seeds to Adsorb Heavy Metals from Aqueous Solution. *J. Ecol. Eng.* **2024**, *25*, 99–118. https://doi.org/10.12911/22998993/189862.
56. Reddy, D.H.K.; Seshaiah, K.; Reddy, A.; Rao, M.M.; Wang, M. Biosorption of Pb^{2+} from aqueous solutions by Moringa oleifera bark: Equilibrium and kinetic studies. *J. Hazard. Mater.* **2010**, *174*, 831–838. https://doi.org/10.1016/j.jhazmat.2009.09.128.
57. Xu, G.; Zhang, Z.; Deng, L. Adsorption Behaviors and Removal Efficiencies of Inorganic, Polymeric and Organic Phosphates from Aqueous Solution on Biochar Derived from Sewage Sludge of Chemically Enhanced Primary Treatment Process. *Water* **2018**, *10*, 869. https://doi.org/10.3390/w10070869.
58. Fan, L.; Wang, X.; Miao, J.; Liu, Q.; Cai, J.; An, X.; Chen, F.; Cheng, L.; Chen, W.; Luo, H.; et al. $Na_4P_2O_7$-Modified Biochar Derived from Sewage Sludge: Effective Cu(II)-Adsorption Removal from Aqueous Solution. *Adsorpt. Sci. Technol.* **2023**, *2023*, 8217910. https://doi.org/10.1155/2023/8217910.

59. Regkouzas, P.; Diamadopoulos, E. Adsorption of selected organic micro-pollutants on sewage sludge biochar. *Chemosphere* **2019**, *224*, 840–851. https://doi.org/10.1016/j.chemosphere.2019.02.165.
60. Yan, L.; Dong, F.-X.; Lin, X.; Zhou, X.-H.; Kong, L.-J.; Chu, W.; Diao, Z.-H. Insights into the removal of Cr(VI) by a biochar–iron composite from aqueous solution: Reactivity, kinetics and mechanism. *Environ. Technol. Innov.* **2021**, *24*, 102057. https://doi.org/10.1016/j.eti.2021.102057.